remote sensing

MDPI

Article

Evaluation and Comparison of ICESat-2 and GEDI Data for Terrain and Canopy Height Retrievals in Short-Stature Vegetation

Xiaoxiao Zhu [1,2,3,4], Sheng Nie [4,5,*], Yamin Zhu [6], Yiming Chen [7], Bo Yang [7] and Wang Li [2]

1 State Key Laboratory of Earthquake Dynamics, Institute of Geology, China Earthquake Administration, Beijing 100029, China; zhuxx@ies.ac.cn
2 State Key Laboratory of Remote Sensing Science, Aerospace Information Research Institute, Chinese Academy of Sciences, Beijing 100101, China; liwang@aircas.ac.cn
3 Key Laboratory of Seismic and Volcanic Hazards, Institute of Geology, China Earthquake Administration, Beijing 100029, China
4 Key Laboratory of Digital Earth Science, Aerospace Information Research Institute, Chinese Academy of Sciences, Beijing 100094, China
5 International Research Center of Big Data for Sustainable Development Goals, Beijing 100094, China
6 Zhejiang Academy of Surveying and Mapping, Hangzhou 311100, China; 2011301130047@whu.edu.cn
7 China Forestry Group Corporation, Beijing 100036, China; chenym@cfgc.cn (Y.C.); yangb@cfgc.cn (B.Y.)
* Correspondence: niesheng@aircas.ac.cn

Abstract: Two space-borne light detection and ranging (LiDAR) missions, Global Ecosystem Dynamics Investigation (GEDI) and Ice, Cloud, and land Elevation Satellite-2 (ICESat-2), have demonstrated high capabilities in extracting terrain and canopy heights in forest environments. However, there have been limited studies evaluating their performance for terrain and canopy height retrievals in short-stature vegetation. This study utilizes airborne LiDAR data to validate and compare the accuracies of terrain and canopy height retrievals for short-stature vegetation using the latest versions of ICESat-2 (Version 5) and GEDI (Version 2). Furthermore, this study also analyzes the influence of various factors, such as vegetation type, terrain slope, canopy height, and canopy cover, on terrain and canopy height retrievals. The results indicate that ICESat-2 (bias = −0.05 m, RMSE = 0.67 m) outperforms GEDI (bias = 0.39 m, RMSE = 1.40 m) in terrain height extraction, with similar results observed for canopy height retrievals from both missions. Additionally, the findings reveal significant differences in terrain and canopy height retrieval accuracies between ICESat-2 and GEDI data under different data acquisition scenarios. Error analysis results demonstrate that terrain slope plays a pivotal role in influencing the accuracy of terrain height extraction for both missions, particularly for GEDI data, where the terrain height accuracy decreases significantly with increasing terrain slope. However, canopy height has the most substantial impact on the estimation accuracies of GEDI and ICESat-2 canopy heights. Overall, these findings confirm the strong potential of ICESat-2 data for terrain and canopy height retrievals in short-stature vegetation areas, and also provide valuable insights for future applications of space-borne LiDAR data in short-stature vegetation-dominated ecosystems.

Keywords: ICESat-2; GEDI; space-borne LiDAR; terrain height; canopy height; short-stature vegetation

Citation: Zhu, X.; Nie, S.; Zhu, Y.; Chen, Y.; Yang, B.; Li, W. Evaluation and Comparison of ICESat-2 and GEDI Data for Terrain and Canopy Height Retrievals in Short-Stature Vegetation. *Remote Sens.* **2023**, *15*, 4969. https://doi.org/10.3390/rs15204969

Academic Editors: Markus Hollaus, Jie Shao, Yiming Chen and Lei Luo

Received: 11 September 2023
Revised: 2 October 2023
Accepted: 9 October 2023
Published: 15 October 2023

1. Introduction

Accurate measurements of terrain and canopy heights play a pivotal role in estimating vegetation carbon stocks, enhancing terrain models to regulate ecosystem responses, and mapping habitat [1,2]. Therefore, the rapid and accurate retrieval of vegetation canopy surfaces and the underlying topography is essential for gaining a deeper understanding of terrestrial ecosystems' functions and services [3]. Light detection and ranging (LiDAR) has become a reliable technique for characterizing surface topography and vertical canopy structure as it can provide detailed and precise three-dimensional information about surface objects [4–6]. However, neither terrestrial nor airborne LiDARs are suitable for large-scale

observations of terrestrial ecosystems due to their high data acquisition costs. In contrast, monitoring the terrain elevation and vertical canopy structure on a large spatial scale is best achieved through space-borne LiDAR technology [7,8].

The Ice, Cloud, and land Elevation Satellite (ICESat) pioneered the use of space-borne LiDAR technology in measuring Earth's surface topography and vegetation canopy height [9,10]. Nevertheless, ICESat concluded its mission in 2009. To continue monitoring changes in Earth's surface elevation globally, the United States successively launched two new space-borne LiDAR missions (Global Ecosystem Dynamics Investigation (GEDI) and ICESat-2) in 2018. ICESat-2 is equipped with the Advanced Topographic Laser Altimeter System (ATLAS) that adopts multi-beam micro-pulse photon counting technology [11]. Compared to its predecessor, ICESat-2/ATLAS offers improved global observation capabilities for vertical canopy structure due to its smaller footprint diameter and higher sampling density [12–14]. GEDI is equipped with the world's first multi-beam full-waveform LiDAR system that is meticulously crafted for precise estimation of vegetation canopy height and biomass [15–17]. The GEDI mission anticipates collecting over 10 billion high-quality full-waveform LiDAR samples.

Recent studies have conducted preliminary evaluations of ICESat-2 and GEDI data performance in extracting terrain and canopy heights in vegetation ecosystems [18–30]. For example, Wang et al. (2019) evaluated the precision of ICESat-2 terrain heights in Alaska's interior using airborne LiDAR data [18]. Their findings indicated a root mean square error (RMSE) value of 1.96 m for terrain height estimates. Neuenschwander et al. (2020) performed an accuracy evaluation of ICESat-2 terrain and canopy height products in boreal forests of southern Finland utilizing airborne LiDAR data acquired from 2008 to 2019, reporting RMSE values of approximately 0.73 m and 3.05 m, respectively [20]. Pourrahmati et al. (2023) verified the accuracy of GEDI in estimating forest heights using airborne LiDAR data collected from 2014 to 2019 in Thuringia, Germany, and reported RMSE values of 6.61 m, 8.30 m, and 7.94 m for coniferous, broad-leaved, and mixed forests, respectively [28]. Additionally, Liu et al. (2021) evaluated and compared ICESat-2 and GEDI's capabilities in terrain and canopy height retrieval using airborne LiDAR data collected in the United States in 2019 [23]. Their results showed RMSE values of 2.24 m and 4.03 m for ICESat-2 and GEDI terrain heights, and 7.21 m and 5.02 m for canopy heights, respectively.

In summary, prior research has shown the significant potential of ICESat-2 and GEDI data in terrain and canopy height extraction, primarily focusing on the forest environment dominated by tall and woody vegetation. However, less attention has been paid to ecosystems dominated by short-stature vegetation, including rangelands (i.e., grasslands, shrublands, and savannas), wetlands (i.e., mangroves, bogs, and swamps), and polar ecosystems (i.e., tundra and taiga). These ecosystems play a key role in many important ecological processes [31,32]. For example, approximately 50% of the world's land area is covered by rangelands that account for more than one-third of terrestrial carbon stocks. Furthermore, LiDAR signals for canopy and ground in areas with short-stature vegetation are susceptible to aliasing, making it challenging to measure surface topography and canopy vertical structure. Therefore, the applicability of these two missions in terrain and canopy height retrieval for short-stature vegetation deserves thorough investigation.

This study aims to evaluate the capability of ICESat-2 and GEDI data in extracting terrain and canopy height over ecosystems dominated by short-stature vegetation. The main contributions of this study include: (1) to extend the potential application of ICESat-2 and GEDI data by focusing on ecosystems dominated by short-stature vegetation, addressing a previously overlooked research area; (2) to rigorously evaluate and compare the accuracy of terrain and canopy height extraction from ICESat-2 and GEDI under various data acquisition scenarios, providing essential insights into their capabilities in short-stature vegetation-dominated environments; and (3) to investigate the influence of various factors on terrain and canopy height extraction in short-stature vegetation ecosystems, offering valuable guidance for future applications of ICESat-2 and GEDI data in such environments.

2. Materials and Methods

2.1. Study Area

We meticulously selected 18 sites from the National Ecological Observatory Network (NEON) as our primary study area (Figure 1). This selection was predicated on the following factors: (1) availability of publicly accessible airborne and space-borne LiDAR datasets across these 18 sites; (2) ability to encompass an array of short-stature vegetation types, including shrubs, grasslands, wetlands, and cultivated lands, thus rendering the study area ecologically diverse; and (3) ability to encompass a spectrum of topographical and climatic conditions, thereby offering a comprehensive range of terrain and climate scenarios for our investigation.

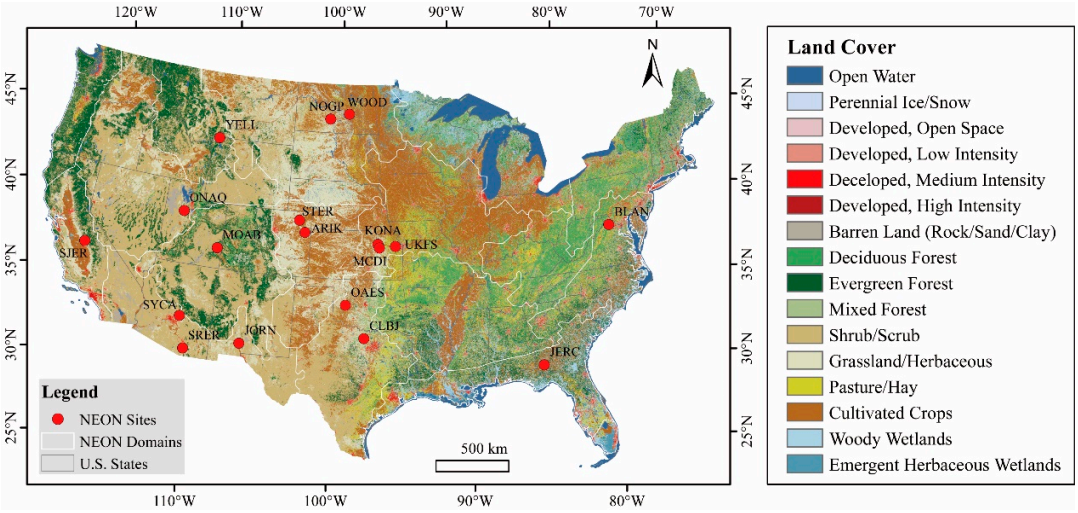

Figure 1. The locations and distribution of the 18 NEON sites used in this study.

2.2. Data

2.2.1. GEDI Data

The GEDI mission was specifically designed to observe the vertical structure and biomass of vegetation on the Earth's surface [33]. GEDI is operated at an orbit altitude of approximately 400 km and emits pulses with a wavelength of 1064 nm, a frequency of 242 Hz, and a pulse width of 14 ns. These specifications produce GEDI footprints with a diameter of around 25 m and an interval of 60 m along its track. GEDI incorporates three lasers capable of generating eight beams (four full-power and four coverage beams). The strip scan width and cross-track distance of GEDI are approximately 4.2 km and 600 m, respectively.

The GEDI products are categorized into seven distinct levels, namely L1A, L1B, L2A, L2B, L3, L4A and L4B. In this study, we downloaded the L2A (Version 2) product collected from April 2019 to December 2022 from the website (https://search.earthdata.nasa.gov/, accessed on 21 March 2023) for subsequent analysis. From the L2A products, we extracted terrain elevation metrics and relative height (RH) metrics (RH80~RH100) for each footprint.

2.2.2. ICESat-2 Data

ICESat-2 boasts the capability to monitor changes in the Earth's surface elevation across a vast range from 88°S to 88°N. The ATLAS system on the ICESat-2 satellite features two lasers, and typically only one laser remains operational at a given time. The ATLAS laser emits pulses at a wavelength of 532 nm, a frequency of 10 kHz, and a pulse width of 1.5 ns. This combination results in overlapping footprints with a diameter of approximately 12 m and an along-track spacing of 0.7 m. The ATLAS system is structured with a total of six laser beams arranged into three groups. Each group comprises a strong and a weak beam with an energy ratio of 4:1. The cross-track distances between inter-group and intra-group beams are approximately 3.3 km and 90 m, respectively [34].

ICESat-2 has 21 data products (ATL01~ATL23). Only the ATL08 product (Version 5) collected from January 2019 to December 2022 was acquired via the website (https://search.earthdata.nasa.gov/, accessed on 21 March 2023). From the ATL08 data, we extracted some metrics, including terrain elevation and RH metrics at various percentiles, namely RH80, RH85, RH90, RH95, RH98, and RH100 [35].

2.2.3. Airborne LiDAR Data

The NEON is a large-scale ecosystem observation network that is strategically designed for the systematic collection of long-term, openly accessible ecological data. The NEON airborne LiDAR data are acquired using the Airborne Laser Terrain Mapper (ALTM) Gemini LiDAR sensor that operates at a wavelength of 1064 nm and a pulse repetition frequency of 100 kHz [36,37].

NEON LiDAR-derived data products encompass digital terrain model (DTM) and canopy height model (CHM). DTM mainly furnishes information regarding terrain elevation and slope, while CHM primarily delineates the relative height of the canopy top above the terrain surface. These two products are archived in GeoTIFF raster format with 1-m resolution, utilizing the ITRF00 datum and projection onto the UTM coordinate system. DTM values are given in meters within the NAVD88 (Geoid12A realization) reference frame [38,39].

To capture the evolving landscape of NEON sites, airborne LiDAR data collection is conducted at intervals ranging from 1 to 5 years. To ensure an ample dataset, we selected the CHMs and DTMs corresponding to 18 NEON sites collected from 2019 to 2022. Table 1 presents a comprehensive overview of the data collection for these 18 NEON sites during the specified timeframe.

Table 1. The availability of 18 NEON sites spanning from 2019 to 2022.

NEON Sites	Year			
	2019	2020	2021	2022
AZ-D14-SRER	√	--	√	--
AZ-D14-SYCA	√	--	√	--
CA-D17-SJER	√	--	√	--
CO-D10-ARIK	--	√	√	√
CO-D10-STER	--	--	√	√
GA-D03-JERC	√	--	√	--
KS-D06-KONA	√	√	--	--
KS-D06-MCDI	--	√	--	--
KS-D06-UKFS	√	√	--	--
ND-D09-NOGP	√	√	√	--
ND-D09-WOOD	√	√	√	--
NM-D14-JORN	√	--	√	--
OK-D11-OAES	√	--	√	√
TX-D11-CLBJ	√	--	√	√
UT-D13-MOAB	√	√	√	√
UT-D15-ONAQ	√	--	√	√
VA-D02-BLAN	√	--	√	√
WY-D12-YELL	√	√	--	√

The names of NEON sites are composed of the abbreviations of U.S. states, domain names, and site names. √ indicates the availability of NEON LiDAR data for the corresponding year. -- indicates the absence of NEON LiDAR data for the corresponding year.

2.2.4. Ancillary Data

The National Land Cover Database (NLCD) stands as the most comprehensive land cover database available to date [40]. NLCD is a 30-m Landsat-based land cover database, encompassing eight different epochs (2001, 2004, 2006, 2008, 2011, 2013, 2016, and 2019). For this study, we employed NLCD 2019 data (USGS/NLCD_RELEASES/2019_REL/NLCD), which is

readily accessible through the Google Earth Engine (GEE) platform to obtain GEDI and ICESat-2 data associated with regions predominantly characterized by short-stature vegetation.

Additionally, this study utilizes the Shuttle Radar Topography Mission (SRTM) DEM (USGS_SRTMGL1_003) shared by the GEE platform to calculate the terrain slope for error analysis. The SRTM space shuttle operates at an orbital altitude of 233 km with an orbital inclination of 57°. Its coverage spans from 60°N to 56°S, effectively encompassing approximately 80% of the Earth's land surface [41]. The spatial resolution of the SRTM DEM is 1 arc second, equivalent to approximately 30 m.

2.3. Space-Borne LiDAR Processing for Terrain and Canopy Height Retrievals

To ensure the reliability of our study, it is imperative to conduct data filtering before extracting terrain and canopy heights from GEDI and ICESat-2 data. For this study, we selected the high-quality GEDI data for subsequent analysis based on the following five criteria: (1) the quality flag must be equal to 1 (quality_flag = 1); (2) the difference between the maximum and minimum terrain heights obtained from six algorithms should be less than 2 m [15,23,42]; (3) the absolute difference between GEDI terrain height and the SRTM DEM should not exceed 50 m; (4) GEDI data must be distributed in short-stature vegetation areas, as indicated by a corresponding NLCD classification value exceeding 50 [40]; and (5) GEDI canopy height should be less than 5 m. Similarly, ICESat-2 data were filtered using the following four criteria: (1) the quality flag "h_canopy_uncertainty" should be less than 20 [23]; (2) the absolute difference between ICESat-2 terrain height and the SRTM DEM should not exceed 50 m; (3) ICESat-2 data should be located in areas with short-stature vegetation, as indicated by a NLCD classification value greater than 50 [40]; and (4) ICESat-2 canopy height should be less than 5 m.

After data filtering, we extracted the parameter "elev_lowestmode" (denoted as the elevation of center of the lowest mode relative to reference ellipsoid) from the GEDI L2A product to stand for the GEDI terrain height. Furthermore, certain RH metrics (RH80~RH100) were extracted from the L2A product. These RH metrics were systematically compared with reference canopy heights obtained from airborne LiDAR to identify the most congruent metric, thus representing GEDI canopy height. Likewise, we employed the parameter "h_te_bestfit" (denoted as the best-fit terrain height at the midpoint of each 100-m segment) from the ATL08 product as the proxy for ICESat-2 terrain height. Regarding canopy height, the RH metric that exhibited the highest level of consistency with airborne LiDAR-derived canopy height was determined to represent ICESat-2 canopy height.

2.4. Airborne LiDAR Processing for Reference Terrain and Canopy Height Extraction

To verify the accuracies of terrain and canopy heights of short-stature vegetation extracted from GEDI and ICESat-2 data, we extracted the reference terrain and canopy heights based on NEON LiDAR DTM and CHM products through the following steps:

- Space-borne LiDAR data buffer zone extraction: For GEDI data, we created a circular buffer zone with a diameter of 25 m centered on the GEDI footprint. Simultaneously, we generated a rectangular buffer zone, spanning 100 m along the ATL08 track and 12 m perpendicular to the track, around the midpoint of the ICESat-2 ATL08 segment.
- DTM and CHM values extraction: Within these buffer zones, we extracted all DTM and CHM values and sorted the CHM values in ascending order.
- Reference elevation and canopy height extraction: The reference terrain elevation was extracted based on the DTM values within the buffer zone. The 95th percentile canopy height was calculated based on the sorted CHM values and employed as the reference canopy height. Additionally, the canopy cover was calculated as the proportion of CHM values greater than 2 m to all CHM values for error analysis.

It is noteworthy that NEON LiDAR DTM and space-borne LiDAR data employ different vertical datums. Specifically, NEON LiDAR DTM uses the North American vertical datum NAVD88 (Geoid12A), whereas both ICESat-2 and GEDI data utilize the WGS84 vertical datum. Consequently, the vertical datum conversion was necessary. To address

this issue, we utilized the National Oceanic and Atmospheric Administration's (NOAA) Vdatum v4.5.1 tool, which offers a solution for transforming data across different vertical datums [43]. This tool facilitated the conversion of the NEON LiDAR DTM's vertical datum from NAVD88 to the WGS84 vertical datum.

2.5. Accuracy Validation

To quantitatively assess the accuracies of terrain and canopy heights derived from GEDI and ICESat-2 data, we employed four statistical indicators: bias, standard deviation (σ), RMSE, and the percent RMSE (%RMSE), as shown in Equations (1)–(4).

Additionally, the accuracies of terrain and canopy heights may differ for different beams (full-power/coverage or strong/weak beam) and acquisition times (night/day) [23,42]. To comprehensively assess these variations, we validated the accuracies of terrain and canopy heights across four different data acquisition scenarios (night/daytime, power/coverage, or strong/weak beam).

$$\text{bias} = \frac{\sum_{i=1}^{n} (x_i - y_i)}{n} \tag{1}$$

$$\sigma = \sqrt{\frac{\sum_{i=1}^{n} (r_i - \bar{r})^2}{n}} \tag{2}$$

$$\text{RMSE} = \sqrt{\frac{\sum_{i=1}^{n} (y_i - x_i)^2}{n-1}} \tag{3}$$

$$\%\text{RMSE} = \frac{\text{RMSE}}{\bar{y}} \cdot 100\% \tag{4}$$

where y_i represents the i_{th} reference terrain or canopy height extracted from the airborne LiDAR data, x_i stands for the i_{th} terrain or canopy height extracted from the space-borne LiDAR data, and r_i denotes the i_{th} terrain or canopy height residual between space-borne LiDAR and airborne LiDAR. $\bar{r}$ is the average value of r_i, $\bar{y}$ is the average of the reference terrain or canopy heights extracted from airborne LiDAR data, and n represents the sample size.

2.6. Error Factor Analysis

In this study, random forest (RF) models were established by using the "ee.Classifier.smileRandomForest()" function in GEE to investigate the impact of various factors on terrain and canopy height retrievals in areas dominated by short-stature vegetation. The parameter "numberOfTrees" in this function was set to 100. The RF models were equipped with a feature that provides the importance levels of error factors through the "explain()" function in GEE. Higher importance value indicates greater significance of the factor. Through the importance values, we can pinpoint the dominant factor affecting the terrain and canopy height errors, thus providing valuable insights for the retrieval and correction of terrain and canopy heights [44,45]. To facilitate the comparison of the importance of various error factors, the relative importance value for each factor was calculated by dividing the importance value of each factor by the maximum importance value.

Additionally, this study further comprehensively assessed the influence of the four aforementioned factors on terrain and canopy height retrievals from ICESat-2 and GEDI data in short-stature vegetation by analyzing the patterns of variation in terrain and canopy height errors associated with each of these factors.

3. Results

3.1. Terrain Height Accuracy

The terrain heights obtained from airborne LiDAR data were employed as reference data to assess the accuracy of terrain heights derived from ICESat-2 and GEDI. Figure 2 illustrates the histogram distribution of terrain height residuals for both missions. Notably, the ICESat-2 terrain height residuals exhibited a more concentrated distribution, primarily falling within the range of −1 m to 1 m. In contrast, the GEDI terrain height residuals were distributed within a broader range of −3 m to 3 m.

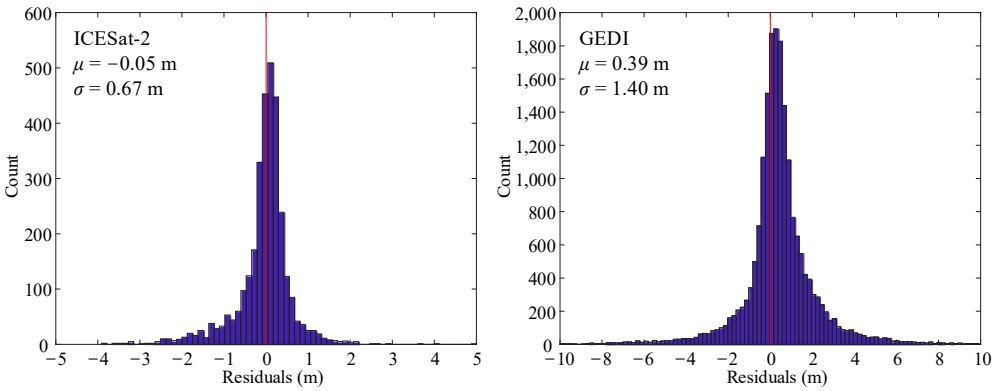

(**a**) (**b**)

Figure 2. Histogram distribution of terrain height residuals for (**a**) ICESat-2 and (**b**) GEDI data. The red line represents the location where the terrain height residual is 0.

Figure 3 presents the verification results for ICESat-2 and GEDI terrain heights across different data acquisition scenarios. The ICESat-2-derived terrain heights exhibited minimal deviation from the reference terrain height with a bias value of only −0.05 m, while GEDI-derived terrain heights tended to be overestimated with a bias value of 0.39 m. Notably, ICESat-2 terrain height accuracy (RMSE = 0.67 m) outperformed that of GEDI (RMSE = 1.40 m). Additionally, Figure 3 also reveals variations in the accuracies of ICESat-2 and GEDI terrain height estimates across different data acquisition scenarios (day/night, strong/weak beams, or full-power/coverage beams). Specifically, the accuracy of ICESat-2 terrain height estimates acquired during daytime (RMSE = 0.83 m) was lower than that acquired at night (RMSE = 0.58 m), whereas the accuracy of GEDI terrain heights estimates remained nearly consistent regardless of day (RMSE = 1.44 m) or night (RMSE = 1.37 m) acquisitions. For GEDI, the terrain height error of strong beams (RMSE = 1.39 m) was significantly smaller than that of weak beams (RMSE = 1.62 m), while little difference existed in terrain height errors between ICESat-2 strong (RMSE = 0.68 m) and weak beams (RMSE = 0.62 m).

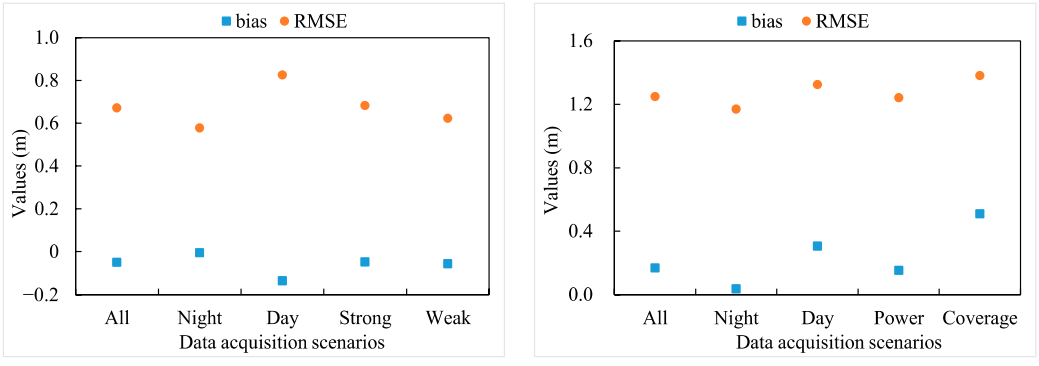

(**a**) (**b**)

Figure 3. The statistical results of terrain height extraction errors for (**a**) ICESat-2 and (**b**) GEDI.

3.2. Canopy Height Accuracy

Various RH metrics extracted from space-borne LiDAR data were compared with reference canopy heights to determine the optimal RH metric as the proxy of canopy height, and the relevant results are illustrated in Figure 4. Notably, the bias was closest to zero and the RMSE value was the smallest when using ICESat-2's RH95 metric. Therefore, the RH95 extracted from ICESat-2 data had the highest correlation with the reference canopy height. Additionally, the results also indicated that the GEDI RH95 performed best as the proxy of canopy height as indicated by its smallest bias and RMSE values.

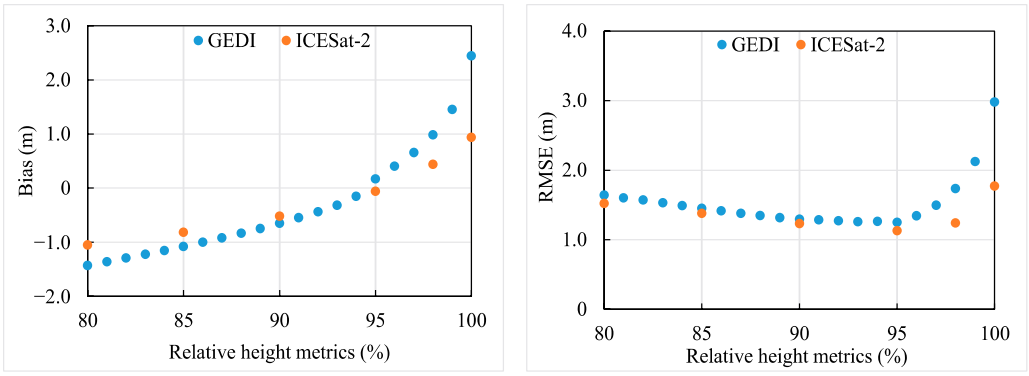

(**a**) (**b**)

Figure 4. Statistical results of relative canopy height extracted from space-borne LiDAR data and airborne LiDAR data: (**a**) Bias and (**b**) RMSE.

The histogram distribution of canopy height residuals for ICESat-2 and GEDI is shown in Figure 5. In contrast to the histogram of terrain height residuals, the distribution of the histogram of canopy height residuals was more scattered. Specifically, the ICESat-2 canopy height residuals were predominantly clustered within the range of −3 m to 3 m, while the GEDI canopy height residuals were primarily distributed within the range of −4 m to 4 m.

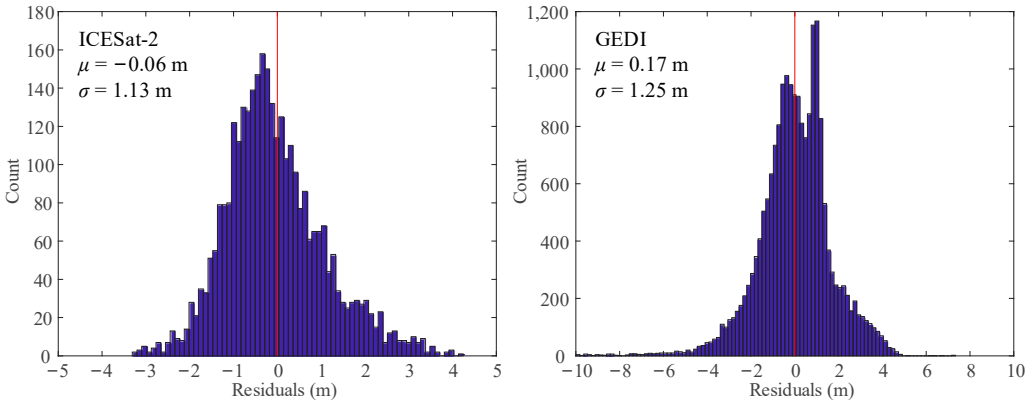

(**a**) (**b**)

Figure 5. Histogram distribution of canopy height residuals for (**a**) ICESat-2 and (**b**) GEDI. The red line represents the location where the canopy height residual is 0.

The verification results for canopy heights extracted from ICESat-2 and GEDI data under different scenarios are shown in Figure 6. The bias between ICESat-2-derived canopy heights and those from airborne LiDAR was close to 0. However, GEDI canopy heights were slightly overestimated when compared to airborne LiDAR-derived canopy heights, with a bias of 0.17 m. The RMSE and %RMSE values for ICESat-2 canopy height (RMSE = 1.13 m; %RMSE = 38%) were lower than that of GEDI canopy height (RMSE = 1.25 m; %RMSE = 52%).

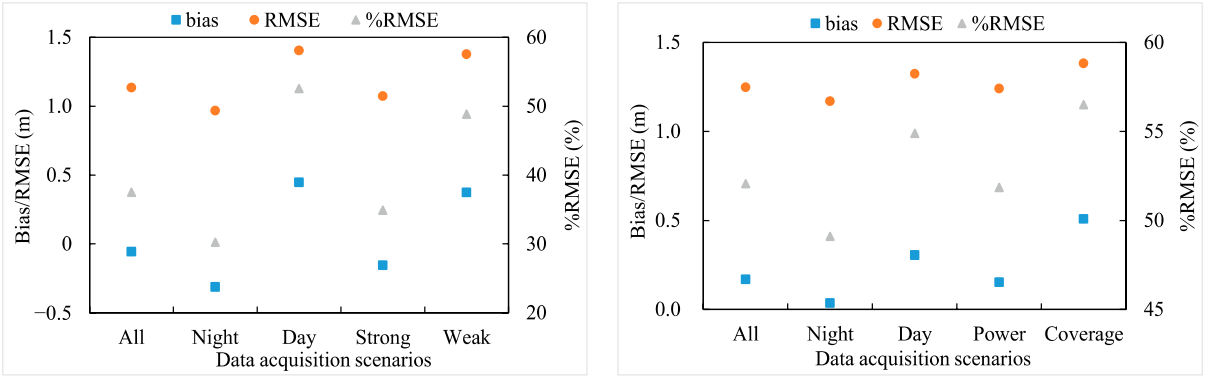

Figure 6. The statistical results of canopy height errors for (**a**) ICESat-2 and (**b**) GEDI.

As observed in Figure 6, the bias, RMSE, and %RMSE values of canopy heights were 0.45 m, 1.41 m, and 53% during the daytime, and −0.31 m, 0.97 m, and 30% at night for ICESat-2 data. In addition, the results in Figure 6 indicate that a difference exists in the canopy height accuracies between strong (bias = −0.15 m; RMSE = 1.07 m; %RMSE = 35%) and weak beams (bias = 0.37 m; RMSE = 1.38 m; %RMSE = 49%). Regarding GEDI data, the accuracy of canopy height extracted during the nighttime (bias = 0.04 m; RMSE = 1.17 m; %RMSE = 49%) was slightly higher than that during the daytime (bias = 0.30 m; RMSE = 1.32 m; %RMSE = 55%). Additionally, GEDI's full-power beams (bias = 0.15 m, RMSE = 1.24 m; %RMSE = 52%) also outperformed the coverage beams (bias = 0.51 m, RMSE = 1.38 m; %RMSE = 57%) in canopy height retrievals.

3.3. Influence of Error Factors on Terrain Height Retrieval

The relative importance of terrain slope, vegetation type, canopy height, and cover in the terrain height extraction from GEDI and ICESat-2 data is shown in Figure 7. It is evident that terrain slope, canopy height, and canopy cover are dominate factors affecting terrain height extraction, irrespective of whether it is GEDI or ICESat-2 data, with vegetation type having the least relative influence. To further analyze the impact of each factor on the terrain height error, we analyzed the patterns of variation in terrain height errors associated with each factor, the relevant results are shown in Figures 8 and 9.

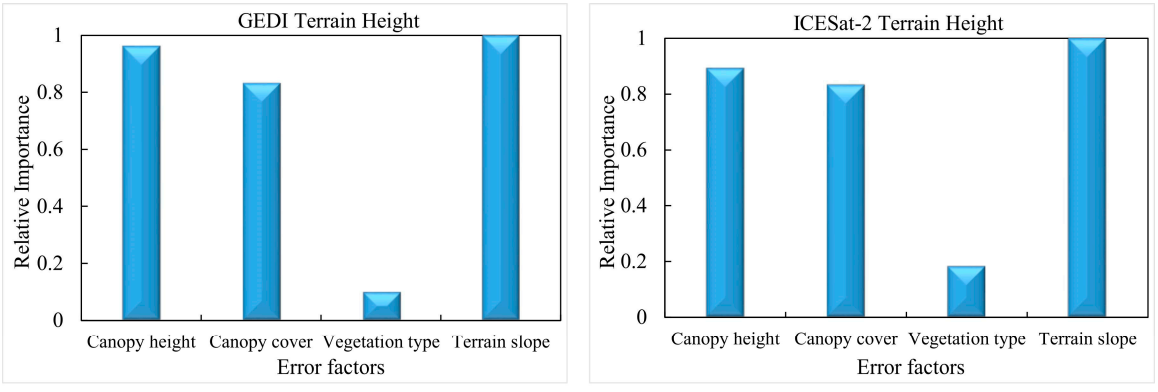

Figure 7. The relative importance of factors in the terrain height extraction for (**a**) GEDI and (**b**) ICESat-2.

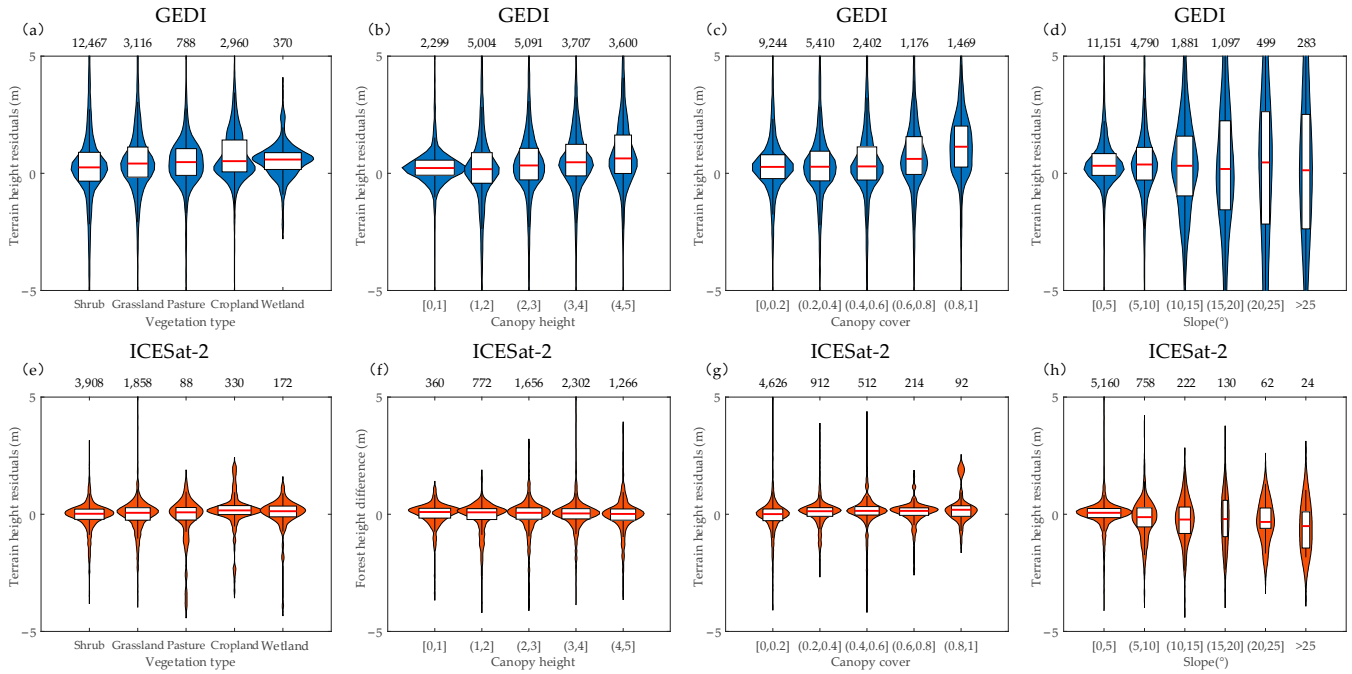

Figure 8. Violin plot of terrain height errors for GEDI (**a**–**d**) and ICESat-2 (**e**–**h**) data grouped by vegetation type (**a**,**e**), canopy height (**b**,**f**), canopy cover (**c**,**g**) and slope (**d**,**h**).

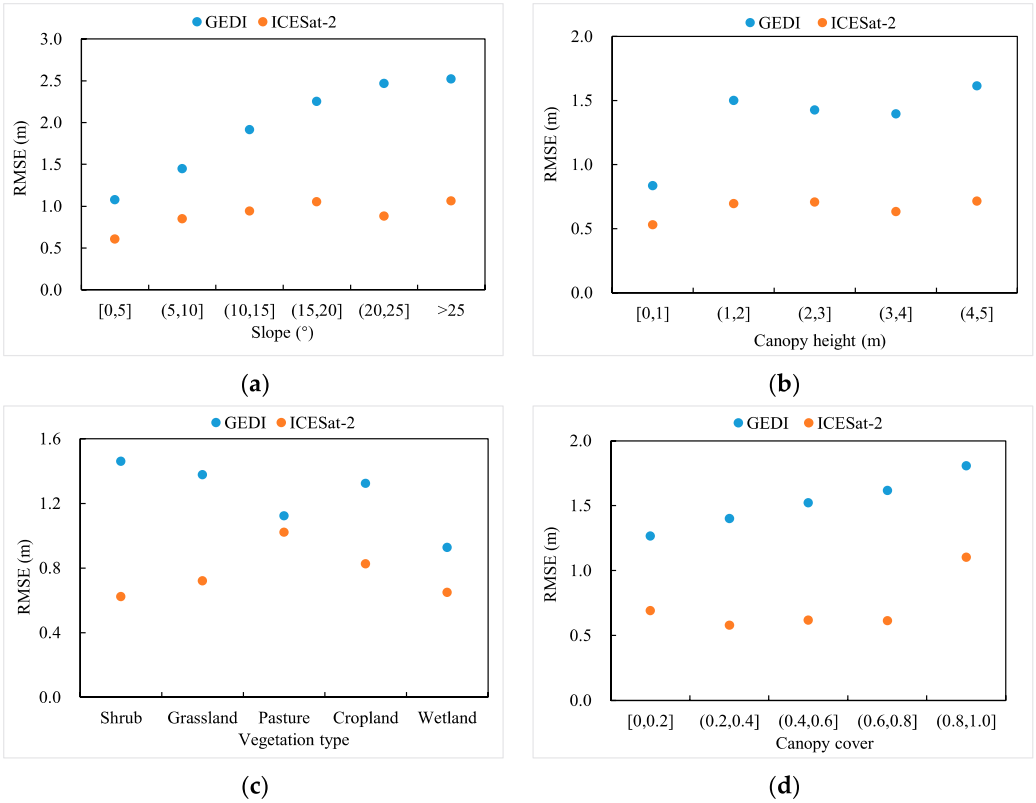

Figure 9. Effects of (**a**) slope, (**b**) canopy height, (**c**) vegetation type and (**d**) canopy cover on terrain height errors of GEDI and ICESat-2 data.

In Figure 8, the violin plots are utilized to illustrate the distribution and probability density of terrain height errors. In these plots, the red horizontal line in the middle indicates the median value, and the shape of the violin plot represents the distribution characteristics of terrain height errors. Figure 8 reveals that the deviation of ICESat-2 terrain height was

more concentrated around zero, while GEDI terrain height exhibited larger deviations, resulting in greater terrain height residuals for GEDI compared to ICESat-2. Consistent with the results shown in the relative importance analysis (Figure 7), the terrain slope had the most significant influence on the terrain height errors, with the range of terrain height residuals gradually expanding as the slope increases. For the GEDI data, the median of terrain height error increased gradually with an increase in canopy height and cover, indicating that the greater canopy height and cover lead to greater overestimates of terrain height. Conversely, the median of ICESat-2 terrain height error gradually decreased as the terrain slope increased.

Figure 9 shows that the RMSE value of GEDI terrain height significantly increased as the terrain slope rose, while the RMSE value of ICESat-2 terrain height remained relatively stable regardless of the terrain slope. When the canopy height did not exceed 1 m, both GEDI and ICESat-2 demonstrated remarkable terrain height accuracy, yielding RMSE values of 0.83 m and 0.53 m, respectively. Additionally, Figure 9 also highlights that the RMSE value of the GEDI terrain height gradually increased with increasing canopy cover, and the RMSE value of ICESat-2 terrain height was highest when the canopy cover exceeded 80%. The terrain height errors for both GEDI and ICESat-2 exhibited variations across various vegetation types. Notably, the RMSE value of ICESat-2 terrain height was less than 1 m for almost all vegetation types.

3.4. Influence of Error Factors on Canopy Height Retrieval

The relative importance of terrain slope, vegetation type, canopy height, and cover in relation to canopy height errors for both GEDI and ICESat-2 data is illustrated in Figure 10. It is evident that canopy height emerged as the most crucial factor influencing the accuracy of vegetation canopy height for both missions. Terrain slope was the second most influential factor affecting GEDI's canopy height retrieval, while ICESat-2's canopy height extraction was minimally impacted by terrain slope.

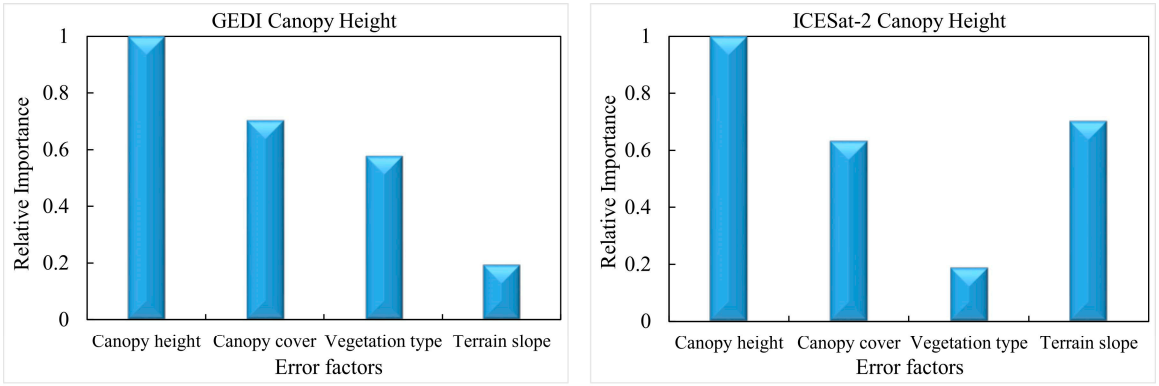

Figure 10. The relative importance of factors in the canopy height extraction for (**a**) GEDI and (**b**) ICESat-2.

Figure 11 demonstrates the relationship between the canopy height errors and each factor. As indicated by Figure 11, the RMSE and %RMSE values of GEDI canopy height exhibited a noticeable upward trend with increasing terrain slope, whereas the RMSE and %RMSE values of ICESat-2 canopy height remained relatively stable despite variations in terrain slope. Furthermore, the canopy height errors for both GEDI and ICESat-2 exhibited variations across different vegetation types. Additionally, the results presented in Figure 11 indicate that the RMSE and %RMSE values of GEDI and ICESat-2 canopy height were at their lowest when the canopy cover and height were at moderate levels.

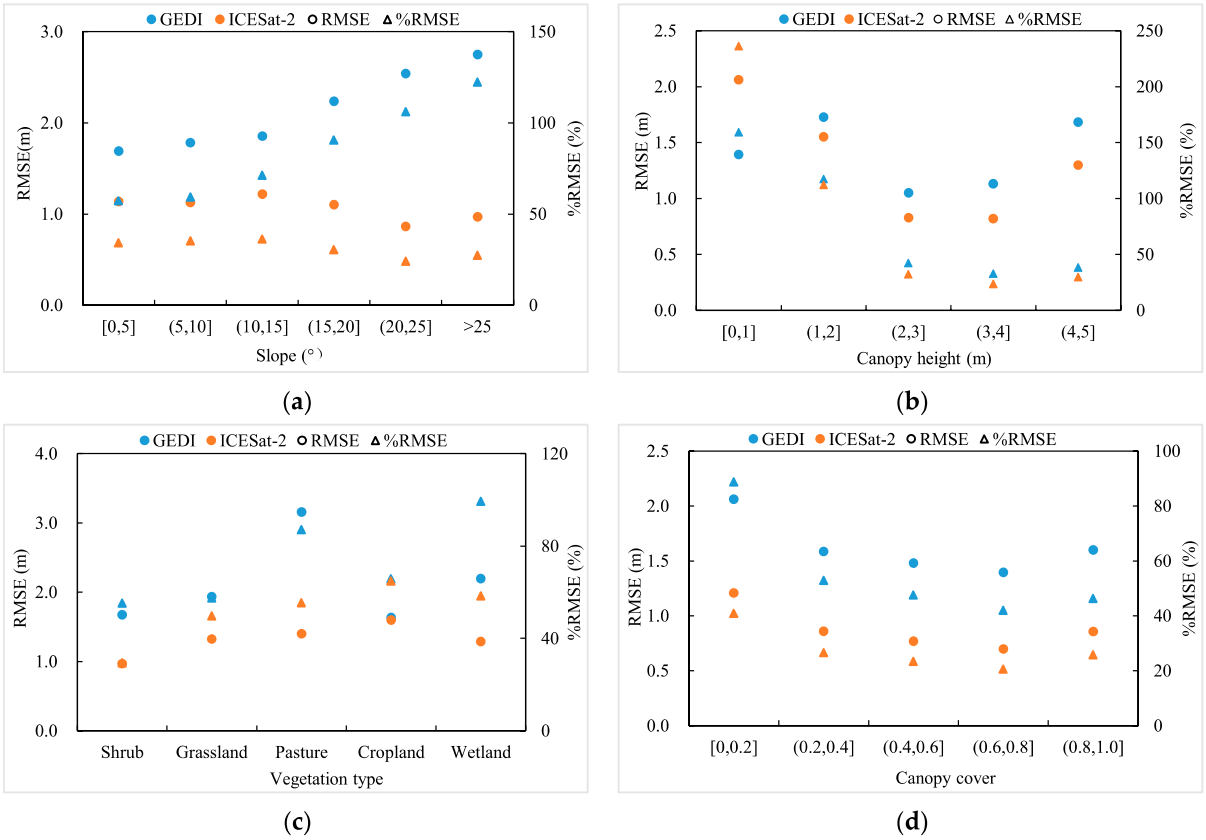

Figure 11. Effects of (**a**) slope, (**b**) canopy height, (**c**) vegetation type and (**d**) canopy cover on canopy height errors of GEDI and ICESat-2 data.

4. Discussion

ICESat-2 and GEDI differ significantly in their measurement principles, measurement scales, and measurement methods for terrain and canopy height [42]. These disparities present considerable challenges when comparing the performance of GEDI and ICESat-2 in extracting terrain and canopy height in areas with short-stature vegetation. While airborne LiDAR also differs from GEDI and ICESat-2 in the aforementioned aspects, it is worth noting that airborne LiDAR has demonstrated strong capabilities in terrain and canopy height measurement. It effectively represents terrain and canopy height within GEDI footprints or ICESat-2 segments, making it a widely used reference for validating the accuracy of terrain and canopy height extractions from GEDI and ICESat-2. To compare the performance of GEDI and ICESat-2 in terrain and canopy height retrievals, airborne LiDAR-derived terrain and canopy height are utilized as reference values. By evaluating the agreement between the estimated values from both GEDI and ICESat-2 with these reference values, we can indirectly compare the performance of GEDI and ICESat-2 in terrain and canopy height extraction.

4.1. Terrain Height Retrieval

The results reveal that ICESat-2 data yield terrain height measurements that demonstrate stronger alignment with the reference terrain height obtained from airborne LiDAR, in comparison to the terrain height extracted from GEDI data. This suggests that ICESat-2 surpasses GEDI in terrain height retrieval over environments characterized by short-stature vegetation. This observation represents a notable departure from prior findings in forested areas, where earlier research predominantly favored GEDI over ICESat-2 in terms of terrain height extraction within vegetative ecosystems [23,42]. Several factors could contribute to this disparity. Firstly, it is plausible that GEDI exhibits larger horizontal positioning errors compared to ICESat-2 [46,47]. Notably, this study did not account for these horizontal

positioning errors. However, we believe that this is not the primary factor influencing the observed results. ICESat-2 consistently maintains higher terrain height accuracy compared to GEDI even in flat terrain where both ICESat-2 and GEDI encounter minimal horizontal positioning errors. Secondly, the substantial pulse width (14.6 ns) of GEDI stands as a prominent factor behind the lower accuracy of GEDI terrain height measurements. This large pulse width leads to the blending of canopy and ground signals, rendering it challenging to distinguish the actual ground signal in short-stature vegetation areas. Consequently, this contributes to an overestimation of terrain height, thus impacting the accuracy of terrain height extraction with GEDI. In contrast, ICESat-2 employs micro-pulses that enable the effective separation of ground and canopy signals even in the environments characterized by short-stature vegetation. Consequently, ICESat-2 data enable precise terrain height retrieval.

In the case of ICESat-2, nighttime data yield higher terrain height accuracy compared to daytime data, and there is minimal disparity in the capability to retrieve terrain height between the weak and strong beams. Conversely, GEDI terrain height accuracy remains relatively consistent between nighttime and daytime data. However, the GEDI full-power beams demonstrate higher accuracy in terrain height extraction when compared to the coverage beams. This situation can be attributed to two primary factors: (1) ICESat-2 data collected during the daytime introduced a significant amount of solar background noises, making it challenging to distinguish signal photons from noise photons and consequently resulting in large errors in terrain height estimates [42]. In contrast, the solar background noise is significantly weaker in comparison to the GEDI signal, rendering its impact on terrain height retrieval accuracy negligible; and (2) although the energy ratio of ICESat-2's strong beam and weak beam is 4:1, the weak beam can capture sufficient ground photons for accurate terrain height estimation in the short-stature vegetation environments. In contrast, the GEDI's full-power beams exhibit superior canopy penetration capabilities compared to the coverage beams [17,22], resulting in higher terrain height extraction accuracy.

The findings reveal that GEDI terrain height accuracy is notably impacted by terrain slope, with its precision deteriorating rapidly as the slope increases. Conversely, ICESat-2 terrain height accuracy remains remarkably stable regardless of slope variations that consistently deliver sub-meter-level terrain height measurements in environments characterized by short-stature vegetation. This could be attributed to the fact that GEDI ground return tends to broaden in steep terrain [19], making it more challenging to distinguish between ground and canopy returns. Additionally, the influence of horizontal geolocation accuracy is more pronounced in steep terrain, leading to greater terrain height errors. In contrast to GEDI, ICESat-2 can accurately extract ground photons even in steep terrain that ensures sub-meter-level terrain height measurement accuracy.

Furthermore, the results also reveal that whether it is GEDI or ICESat-2, the precision of their terrain height measurements experiences a notable decline under high canopy cover conditions. This decline in accuracy may be attributed to the challenge of accurately discerning ground signals in regions with dense canopy cover that consequently impacts the accuracy of terrain height extraction.

4.2. Canopy Height Retrieval

The findings reveal that the canopy height measurements derived from ICESat-2 data exhibit stronger consistency with the reference canopy height obtained from airborne LiDAR compared to the canopy height extracted from GEDI data. This suggests that ICESat-2 outperforms GEDI in retrieving canopy height for short-stature vegetation. This difference in performance can be attributed in part to the limitations of GEDI in effectively extracting terrain height and partly to inaccuracies in identifying canopy top positions. These inaccuracies arise due to the challenges posed by the overlap of ground and canopy returns in areas with short-stature vegetation. Both of these aspects collectively influence the precision of canopy height extraction from GEDI data.

Furthermore, the results indicate that canopy height is overestimated during the daytime and underestimated at night, with ICESat-2 data collected at night exhibiting higher canopy height extraction accuracy than daytime data. The possible reason for this is that daytime ICESat-2 data introduce a significant amount of noise photons that thereby reduce the accuracy of canopy height extraction [23]. Additionally, ICESat-2's strong beams demonstrate superior canopy height measurement capabilities compared to the weak beams. This can be explained by the higher energy of ICESat-2's strong beam, resulting in the reception of more signal photons and facilitating more precise detection of canopy top positions [42], ultimately leading to higher canopy height extraction accuracy.

The results also indicate that the full-power beams of GEDI exhibit higher canopy height accuracy compared to the coverage beams, and nighttime data yield higher canopy height accuracy than daytime data. Two primary factors contribute to this phenomenon. Firstly, the presence of solar background noise in GEDI waveforms may affect the extraction of canopy top position. Secondly, the GEDI coverage beams have weaker terrain height extraction capabilities that thereby affect their canopy height estimation accuracy [23,42].

Similar to the pattern observed with terrain height being influenced by terrain slope, canopy height accuracy from GEDI decreases significantly when terrain slope is steep, while ICESat-2 maintains high canopy height accuracy. This could be attributed to the fact that increasing slope steepness results in more overlap between ground and canopy returns in GEDI data [27,28], which in turn affects the extraction of canopy height. In contrast, ICESat-2's ground and canopy-top photons are relatively less affected by terrain slope, contributing to its higher canopy height extraction accuracy in steep terrain. Additionally, both GEDI and ICESat-2 exhibit their highest canopy height accuracy when canopy cover and height are within moderate levels. Accurately extracting the position of the ground or canopy-top surface from GEDI and ICESat-2 data becomes challenging when canopy cover is extremely high or low [20,24], thus limiting the precision of canopy height extraction. Conversely, when canopy height falls within a moderate range, the mixing of canopy and ground signals is minimized which ensures high accuracy in canopy height retrieval.

5. Conclusions

This study assessed the effectiveness of both GEDI and ICESat-2 data in extracting terrain and canopy heights in ecosystems characterized by short-stature vegetation. Furthermore, it analyzed the impact of various factors on the accuracy of terrain and canopy height retrievals. The key findings are as follows: (1) ICESat-2 data exhibit sub-meter-level precision in terrain height observations within short-stature vegetation areas, particularly in regions characterized by shrub and wetland distributions, with RMSE values of 0.62 m and 0.65 m, respectively; (2) ICESat-2 outperforms GEDI in the retrieval of terrain and canopy heights in short-stature vegetation environments; (3) the accuracy of terrain and canopy height estimates from ICESat-2 and GEDI data varies depending on the data acquisition scenarios; and (4) terrain slope emerges as the most influential factor affecting the accuracy of terrain height extraction for both GEDI and ICESat-2 data, while canopy height exerts the greatest influence on the retrieval of canopy heights for both missions.

In summary, this study represents an initial exploration of terrain and canopy height extraction using GEDI and ICESat-2 data in ecosystems dominated by short-stature vegetation. The findings will offer valuable insights for the future utilization of ICESat-2 and GEDI data in ecosystems characterized by short-stature vegetation dominance. However, this study has limited its site selection to several NEON sites within the United States and has not taken into account the potential impact of GEDI geolocation error on terrain and canopy height extraction in areas with short-stature vegetation. Future research endeavors should aim to broaden the selection of study sites on a global scale and account for the geolocation error associated with GEDI data.

Author Contributions: Conceptualization, X.Z. and S.N.; methodology, X.Z. and S.N.; software, Y.Z. and W.L.; validation, X.Z. and Y.Z.; investigation, X.Z.; data curation, Y.C., B.Y. and Y.Z.; writing—original draft preparation, X.Z.; writing—review and editing, S.N., Y.C. and B.Y.; visualization, X.Z.; supervision, S.N.; funding acquisition, X.Z., S.N. and W.L. All authors have read and agreed to the published version of the manuscript.

Funding: This research was supported by the Open Research Fund of the Key Laboratory of Digital Earth Science, Aerospace Information Research Institute, Chinese Academy of Sciences (2022LDE002), the Open Fund of the State Key Laboratory of Remote Sensing Science (OFSLRSS202313), National Natural Science Foundation of China (42171352, 42171369), Youth Innovation Promotion Association CAS (2019130), and the National Nonprofit Fundamental Research Grant of China, Institute of Geology, China Earthquake Administration (IGCEA2224).

Data Availability Statement: Not applicable.

Acknowledgments: The authors want to acknowledge NASA for providing ICESat-2 and GEDI data, NEON for airborne LiDAR data, and NOAA for VDatum v4.5.1 software.

Conflicts of Interest: The authors declare no conflict of interest.

References

1. Zhang, G.; Ganguly, S.; Nemani, R.R.; White, M.A.; Milesi, C.; Hashimoto, H.; Wang, W.; Saatchi, S.; Yu, Y.; Myneni, R.B. Estimation of forest aboveground biomass in California using canopy height and leaf area index estimated from satellite data. *Remote Sens. Environ.* **2014**, *151*, 44–56. [CrossRef]
2. Pugh, T.A.M.; Lindeskog, M.; Smith, B.; Poulter, B.; Arneth, A.; Haverd, V.; Calle, L. Role of forest regrowth in global carbon sink dynamics. *Proc. Natl. Acad. Sci. USA* **2019**, *116*, 4382–4387. [CrossRef] [PubMed]
3. Lafortezza, R.; VGiannico, V. Combining high-resolution images and LiDAR data to model ecosystem services perception in compact urban systems. *Ecol. Indic.* **2019**, *96*, 87–98. [CrossRef]
4. Davies, A.B.; Asner, G.P. Advances in animal ecology from 3D-LiDAR ecosystem mapping. *Trends Ecol. Evol.* **2014**, *29*, 681–691. [CrossRef] [PubMed]
5. Hostetler, C.A.; Behrenfeld, M.J.; Hu, Y.X.; Hair, J.W.; Schulien, J.A. Spaceborne lidar in the study of marine systems. *Annu. Rev. Mar. Sci.* **2017**, *10*, 121–147. [CrossRef]
6. Wan, P.; Shao, J.; Jin, S.; Wang, T.; Yang, S.; Yan, G.; Zhang, W. A novel and efficient method for wood–leaf separation from terrestrial laser scanning point clouds at the forest plot level. *Methods Ecol. Evol.* **2021**, *12*, 2473–2486. [CrossRef]
7. Huang, X.; Cheng, F.; Wang, J.; Duan, P.; Wang, J. Forest Canopy Height Extraction Method Based on ICESat-2/ATLAS Data. *IEEE Trans. Geosci. Remote Sens.* **2023**, *61*, 5700814. [CrossRef]
8. Wulder, M.A.; White, J.C.; Nelson, R.F.; Næsset, E.; Ørka, H.O.; Coops, N.C.; Hilker, T.; Bater, C.W.; Gobakken, T. LiDAR sampling for large-area forest characterization: A review. *Remote Sens. Environ.* **2012**, *121*, 196–209. [CrossRef]
9. Lefsky, M.A. A global forest canopy height map from the Moderate Resolution Imaging Spectroradiometer and the Geoscience Laser Altimeter System. *Geophys. Res. Lett.* **2010**, *37*, L15401. [CrossRef]
10. Nie, S.; Wang, C.; Zeng, H.; Xi, X.; Xia, S. A revised terrain correction method for forest canopy height estimation using ICESat/GLAS data. *ISPRS J. Photogramm. Remote Sens.* **2015**, *108*, 183–190. [CrossRef]
11. Neumann, T.A.; Martino, A.J.; Markus, T.; Bae, S.; Bock, M.R.; Brenner, A.C.; Brunt, K.M.; Cavanaugh, J.; Fernandes, S.T.; Hancock, D.W.; et al. The ice, cloud, and land elevation Satellite-2 Mission: A global geolocated photon product derived from the advanced topographic laser altimeter system. *Remote Sens. Environ.* **2019**, *233*, 111325. [CrossRef] [PubMed]
12. Markus, T.; Neumann, T.; Martino, A.; Abdalati, W.; Brunt, K.; Csatho, B.; Farrell, S.; Fricker, H.; Gardner, A.; Harding, D.; et al. The ice, cloud, and land elevation Satellite-2 (ICESat-2): Science requirements, concept, and implementation. *Remote Sens. Environ.* **2017**, *190*, 260–273. [CrossRef]
13. Mulverhill, C.; Coops, N.C.; Hermosilla, T.; White, J.C.; Wulder, M.A. Evaluating ICESat-2 for monitoring, modeling, and update of large area forest canopy height products. *Remote Sens. Environ.* **2022**, *271*, 112919. [CrossRef]
14. Feng, T.; Duncanson, L.; Montesano, P.; Hancock, S.; Minor, D.; Guenther, E.; Neuenschwander, A. A systematic evaluation of multi-resolution ICESat-2 ATL08 terrain and canopy heights in boreal forests. *Remote Sens. Environ.* **2023**, *291*, 113570. [CrossRef]
15. Potapov, P.; Li, X.; Hernandezserna, A.; Tyukavina, A.; Hansen, M.C.; Kommareddy, A.; Pickens, A.; Turubanova, S.; Tang, H.; Silva, C.E.; et al. Mapping and monitoring global forest canopy height through integration of GEDI and landsat data. *Remote Sens. Environ.* **2020**, *253*, 112165. [CrossRef]
16. Schneider, F.; Ferraz, A.; Hancock, S.; Duncanson, L.; Dubayah, R.; Pavlick, R.; Schimel, D. Towards mapping the diversity of canopy structure from space with GEDI. *Environ. Res. Lett.* **2020**, *15*, 115006. [CrossRef]
17. Silva, C.A.; Duncanson, L.; Hancock, S.; Neuenschwander, A.; Thomas, N.; Hofton, M.; Fatoyinbo, L.; Simard, M.; Marshak, C.Z.; Armston, J.; et al. Fusing simulated GEDI, ICESat-2 and NISAR data for regional aboveground biomass mapping. *Remote Sens. Environ.* **2021**, *253*, 112234. [CrossRef]

18. Wang, C.; Zhu, X.; Nie, S.; Xi, X.; Li, D.; Zheng, W.; Chen, S. Ground elevation accuracy verification of ICESat-2 data: A case study in Alaska, USA. *Opt. Express* **2019**, *27*, 38168–38179. [CrossRef]
19. Adam, M.; Urbazaev, M.; Dubois, C.; Schmullius, C. Accuracy assessment of GEDI terrain elevation and canopy height estimates in European temperate forests: Influence of environmental and acquisition parameters. *Remote Sens.* **2020**, *12*, 3948. [CrossRef]
20. Neuenschwander, A.; Guenther, E.; White, J.; Duncanson, L.; Montesano, P. Validation of ICESat-2 terrain and canopy heights in boreal forests. *Remote Sens. Environ.* **2020**, *233*, 111325. [CrossRef]
21. Xing, Y.; Huang, J.; Gruen, A.; Qin, L. Assessing the performance of ICESat-2/ATLAS multi-channel photon data for estimating ground topography in forested terrain. *Remote Sens.* **2020**, *12*, 2084. [CrossRef]
22. Dorado-Roda, I.; Pascual, A.; Godinho, S.; Silva, C.A.; Botequim, B.; Rodríguez-Gonzálvez, P.; González-Ferreiro, E.; Guerra-Hernández, J. Assessing the accuracy of GEDI data for canopy height and aboveground biomass estimates in Mediterranean forests. *Remote Sens.* **2021**, *13*, 2279. [CrossRef]
23. Liu, A.; Cheng, X.; Chen, Z. Performance evaluation of GEDI and ICESat-2 laser altimeter data for terrain and canopy height retrievals. *Remote Sens. Environ.* **2021**, *264*, 112571. [CrossRef]
24. Malambo, L.; Popescu, S.C. Assessing the agreement of ICESat-2 terrain and canopy height with airborne lidar over US ecozones. *Remote Sens. Environ.* **2021**, *266*, 112711. [CrossRef]
25. Fernandez-Diaz, J.C.; Velikova, M.; Glennie, C.L. Validation of ICESat-2 ATL08 Terrain and Canopy Height Retrievals in Tropical Mesoamerican Forests. *IEEE J. Sel. Top. Appl. Earth Obs. Remote Sens.* **2022**, *15*, 2956–2970. [CrossRef]
26. Urbazaev, M.; Hess, L.; Hancock, S.; Sato, L.Y.; Ometto, J.P.; Thiel, C.; Dubois, C.; Heckel, K.; Urban, M.; Adam, M.; et al. Assessment of terrain elevation estimates from ICESat-2 and GEDI spaceborne LiDAR missions across different land cover and forest types. *Sci. Remote Sens.* **2022**, *6*, 100067. [CrossRef]
27. Li, X.; Wessels, K.; Armston, J.; Hancock, S.; Mathieu, R.; Main, R.; Naidoo, L.; Erasmus, B.; Scholes, R. First validation of GEDI canopy heights in African savannas. *Remote Sens. Environ.* **2023**, *285*, 113402. [CrossRef]
28. Pourrahmati, M.R.; Baghdadi, N.; Fayad, I. Comparison of GEDI LiDAR Data Capability for Forest Canopy Height Estimation over Broadleaf and Needleleaf Forests. *Remote Sens.* **2023**, *15*, 1522. [CrossRef]
29. Rodda, S.R.; Nidamanuri, R.R.; Fararoda, R.; Mayamanikandan, T.; Rajashekar, G. Evaluation of Height Metrics and Above-Ground Biomass Density from GEDI and ICESat-2 Over Indian Tropical Dry Forests using Airborne LiDAR Data. *J. Indian Soc. Remote Sens.* **2023**. [CrossRef]
30. Vatandaslar, C.; Narin, O.G.; Abdikan, S. Retrieval of forest height information using spaceborne LiDAR data: A comparison of GEDI and ICESat-2 missions for Crimean pine (*Pinus nigra*) stands. *Trees Struct. Funct.* **2023**, *37*, 717–731. [CrossRef]
31. Allen-Diaz, B. Rangelands in a changing climate: Impacts, adaptations, and mitigation. In *Impacts, Adaptations, and Mitigation of Climate Change: Scientific-Technical Analyses*; Watson, R.T., Zinyowera, M.C., Moss, R.H., Eds.; Climate Change 1995; Cambridge University Press: Cambridge, UK, 1996; pp. 131–158.
32. Kulawardhana, R.W.; Popescu, S.C.; Feagin, R.A. Airborne lidar remote sensing applications in non-forested short stature environments: A review. *Ann. For. Res.* **2017**, *60*, 173–196. [CrossRef]
33. Dubayah, R.; Blair, J.B.; Goetz, S.; Fatoyinbo, L.; Silva, C. The Global Ecosystem Dynamics Investigation: High-resolution laser ranging of the Earth's forests and topography. *Sci. Remote Sens.* **2020**, *1*, 100002. [CrossRef]
34. Neuenschwander, A.; Pitts, K. The ATL08 land and vegetation product for the ICESat-2 Mission. *Remote Sens. Environ.* **2019**, *221*, 247–259. [CrossRef]
35. Neuenschwander, A.; Pitts, K.; Jelley, B.; Robbins, J.; Markel, J.; Popescu, S.; Nelson, R.; Harding, D.; Pederson, D.; Klotz, B.; et al. Ice, Cloud, and Land Elevation Satellite-2 (ICESat-2) Algorithm Theoretical Basis Document (ATBD) for Land-Vegetation Along-Track Products (ATL08). Available online: https://icesat-2.gsfc.nasa.gov/science/data-products (accessed on 25 January 2023).
36. Carrasco, L.; Giam, X.; Papes, M.; Sheldon, K.S. Metrics of Lidar-Derived 3D Vegetation Structure Reveal Contrasting Effects of Horizontal and Vertical Forest Heterogeneity on Bird Species Richness. *Remote Sens.* **2019**, *11*, 743. [CrossRef]
37. Kampe, T.U.; Johnson, B.R.; Kuester, M.A.; Keller, M. NEON: The first continental-scale ecological observatory with airborne remote sensing of vegetation canopy biochemistry and structure. *Proc. SPIE Int. Soc. Opt. Eng.* **2010**, *4*, 043510. [CrossRef]
38. NEON (National Ecological Observatory Network). Ecosystem Structure (DP3.30015.001), RELEASE-2023. Available online: https://data.neonscience.org (accessed on 30 March 2023).
39. NEON (National Ecological Observatory Network). Ecosystem Structure (DP3.30015.001). Available online: https://data.neonscience.org (accessed on 30 March 2023).
40. Yang, L.; Jin, S.; Danielson, P.; Homer, C.; Gass, L.; Bender, S.M.; Case, A.; Costello, C.; Dewitz, J.; Fry, J.; et al. A new generation of the United States National Land Cover Database: Requirements, research priorities, design, and implementation strategies. *ISPRS J. Photogramm. Remote Sens.* **2018**, *146*, 108–123. [CrossRef]
41. Farr, T.G.; Rosen, P.A.; Caro, E.; Crippen, R.; Duren, R.; Hensley, S.; Kobrick, M.; Paller, M.; Rodriguez, E.; Roth, L.; et al. The shuttle radar topography mission. *Rev. Geophys.* **2007**, *45*, RG2004. [CrossRef]
42. Zhu, X.; Nie, S.; Wang, C.; Xi, X.; Lao, J.; Li, D. Consistency analysis of forest height retrievals between GEDI and ICESat-2. *Remote Sens. Environ.* **2022**, *281*, 113244. [CrossRef]
43. Parker, B.; Hess, K.W.; Milbert, D.G.; Gill, S. A national vertical datum transformation tool. *Sea Technol.* **2003**, *44*, 10–15.
44. Wang, C.; Elmore, A.J.; Numata, I.; Cochrane, M.A.; Lei, S.; Huang, J.; Zhao, Y.; Li, Y. Factors affecting relative height and ground elevation estimations of GEDI among forest types across the conterminous USA. *GISci. Remote Sens.* **2022**, *59*, 975–999. [CrossRef]

45. Moudrý, V.; Gdulová, K.; Gábor, L.; Šárovcová, E.; Barták, V.; Leroy, F.; Špatenková, O.; Rocchini, D.; Prošek, J. Effects of environmental conditions on ICESat-2 terrain and canopy heights retrievals in Central European mountains. *Remote Sens. Environ.* **2022**, *279*, 113112. [CrossRef]
46. Tang, H.; Stoker, J.; Luthcke, S.; Armston, J.; Lee, K.; Blair, B.; Hofton, M. Evaluating and mitigating the impact of systematic geolocation error on canopy height measurement performance of GEDI. *Remote Sens. Environ.* **2023**, *291*, 113571. [CrossRef]
47. Xu, Y.; Ding, S.; Chen, P.; Tang, H.; Ren, H.; Huang, H. Horizontal Geolocation Error Evaluation and Correction on Full-Waveform LiDAR Footprints via Waveform Matching. *Remote Sens.* **2023**, *15*, 776. [CrossRef]